IEEE Access
Multidisciplinary | Rapid Review | Open Access Journal

Date of current version: September, 2024

Digital Object Identifier 10.1109/ACCESS.2024.

Dynamic Car-Following Model with Jerk Suppression for Highway Autonomous Driving

KE LIU, JING MA (Member, IEEE) and EDMUND M-K. LAI (Life Senior Member, IEEE)
School of Engineering, Computer and Mathematical Sciences, Auckland University of Technology, Auckland, New Zealand (e-mail: {ke.liu, jing.ma, edmund.lai}@aut.ac.nz)

Corresponding author: Jing Ma (e-mail: jing.ma@aut.ac.nz)

The research of Edmund Lai is partly supported by Project 111 (No. D23006).

ABSTRACT This study proposes a dynamic safe car-following strategy that is based on dynamic adjustment of headway time with jerk suppression. Reinforcement learning models trained with this strategy result in enhanced safety and driving comfort, validated using real driving data from the Next Generation Simulation (NGSIM) I-80 and HighD datasets. Simulation results demonstrate significant reduction in the risk of collisions. More importantly, low collision rates are maintained with driving speed profiles that are different from the training data, exhibiting cross-dataset generalizability. It also significantly improves driving comfort, with a 10% jerk reduction compared to existing models.

INDEX TERMS Autonomous driving; car-following; jerk reduction; adaptive headway threshold

I. INTRODUCTION

Autonomous driving has the potential to significantly enhance traffic safety, driving comfort, and overall road efficiency [1]. One of the most fundamental yet critical driving scenario for autonomous vehicles (AVs) is car-following. In this scenario, an AV drives behind a leading vehicle – a situation common in both urban and highway environments. To ensure safety, the AV must regulate its speed to avoid colliding with the vehicle ahead, while also maintaining a smooth driving experience in changing traffic conditions. Furthermore, minimizing abrupt acceleration changes during the car-following process is essential for enhanced ride comfort. Thus, the car-following task involves not only maintaining an appropriate following distance but also ensuring a safe and comfortable ride [2].

The driving behaviour of the AV is determined by a decision model that controls its acceleration and deceleration [3]. The first car-following model was proposed in the 1950s [4]. Since then, many other models have emerged, including the rule-based Gazis-Herman-Rothery (GHR) model [5], [6], the optimal velocity model [7], and the Intelligent Driving Model (IDM) [8]. These models attempt to mimic human driving behaviour. With the advances in machine learning techniques, more recent efforts are based on data-driven approaches. Feedforward artificial neural network [9], [10] and recurrent neural network [11], [12], models are trained with human driving data to mimic their behaviours. These models learn the nonlinear driving behaviour through recorded human driving data. The quality of such models depends largely on the quality of the training datasets [1]. The collection of training datasets that cover the whole range of speed and acceleration profiles is time-consuming and costly. Furthermore, it is difficult to introduce driving constraints into the training process.

Reinforcement learning (RL) is able to overcome the above limitations. It is a machine learning approach that learns action policies in response to feedback from the environment. Therefore, it has been applied to many different aspects of autonomous driving, including car-following [13]–[15]. In particular, when the action space is continuous, the Deep Deterministic Policy Gradient (DDPG) algorithm, which combines ideas from deep learning and policy gradients to learn complex behaviours, is often used [16]. In [17], a car-following model based on the DDPG algorithm was proposed. Its reward function promotes safety, efficiency, and comfort, the three important aspects of car-following described earlier. However, the safety strategy designed by Zhu et al. [17] relies on a static Time To Collision (TTC) measure. This approach has limitations because it uses a fixed threshold for TTC which does not adapt well to the varying conditions of real-world driving. Furthermore, TTC may not accurately reflect all dangerous situations in car-following, especially when the relative speed between vehicles is low but the following distance is short, leading to high TTC values that still pose significant safety risks.

In this paper, an alternative approach is proposed by using

headway time as the primary metric for measuring safety in car-following scenarios. Unlike TTC, headway time dynamically adapts to varying driving conditions by recalculating the safety threshold based on the real-time car-following situation, making it more robust and better suited to the complexities of real-world driving environments. While previous studies (see [18] for example) have emphasized the importance of incorporating driver behaviour into safety distance calculations, our model focuses on vehicle kinematics to provide a deterministic and reliable control strategy for autonomous vehicles. This choice ensures consistency and predictability in various driving scenarios, which is essential for the safe operation of AVs. In addition, this paper introduces a jerk suppression method which adaptively limits the acceleration and deceleration range of the autonomous vehicle (AV) to enhance ride comfort.

Our work focusses on car-following scenarios on highways. It is also the focus of many other previous studies [17] and is used here to validate our proposed car-following strategy. In urban environments, there are intersections, traffic lights, and other factors that makes the driving environment more complex. They significantly influence driver behaviour, particularly car-following behaviour during braking [19]. In our experiments, the reinforcement learning models are trained with real driving data from the Next Generation Simulation (NGSIM) project [20] and the HighD dataset [21], which implicitly reflects driver behaviours on highways. The results demonstrate that the proposed strategy significantly improves safety, efficiency, and comfort, outperforming existing models across different traffic conditions and datasets.

The rest of this paper is organized as follows. A background research is presented in Section II. It also gives an review of reinforcement model for car-following in Section III. Section IV proposed an improved method with jerk suppression in detail. An evaluation of the performance of improved method has been tested in Section VI. This is followed by Section VII that concludes this article with some suggestions for further research.

II. CAR-FOLLOWING MODELS

Current research has found that complex traffic scenarios can be decomposed into simpler traffic paths and trajectories, such as car-following [17], cut-in [22], and lane-change [23]. Car-following is one of the simplest yet important driving tasks and has received widespread attention from researchers [24]. There are two main categories of models for car-following: traditional and data-driven [25].

A. TRADITIONAL MODELS

Among traditional car-following models, the Gazis-Herman-Rothery (GHR) model [26] and the Intelligent Driver Model (IDM) [8] are representative. The GHR model assumes a positive correlation between vehicle acceleration and speed difference, with the response of the following vehicle expressed through its acceleration or deceleration behaviour. The IDM is a comprehensive and straightforward theoretical model that prioritizes safety and accident prevention. These traditional models still hold value in traffic engineering and flow analysis research. For example, IDM can handle any traffic situation on urban, rural roads, or highways led by manual or autonomous driving, and has even been successfully applied to bicycle traffic flow and mixed traffic flow in developing countries like India [27]. However, traditional models may have several potential drawbacks, such as oversimplifying assumptions about driver behaviour and neglecting individual driving differences or different driving styles.

B. LEARNING-BASED MODELS

Due to recent advances in computation and data collection technologies, more advanced learning-based car-following models have been developed. These models, represented by deep reinforcement learning , can effectively predict driver behaviour by learning the relationships between various factors and driver actions from collected data [28]. For instance, Ren et al. [28] developed an autonomous car-following model based on the Deep Q-Network (DQN) algorithm, achieving precise control and preset improvement goals through training agents in a traffic simulator, significantly improving the performance and reliability of autonomous vehicles in car-following scenarios. Qin et al. [29] proposed a car-following strategy based on the Twin Delayed Deep Deterministic Policy Gradient (TD3) algorithm, designing a multi-objective constrained reward function that comprehensively considers safety, traffic efficiency, and ride comfort. However, while the TD3 algorithm handles continuous action spaces, its limitations in exploration space and slow convergence hinder its performance in real-time car-following tasks, particularly in resource-constrained environments.

In contrast, recent studies have focused on using the Deep Deterministic Policy Gradient (DDPG) algorithm to address these challenges. DDPG not only excels in handling continuous action spaces but also better adapts to complex and dynamic traffic environments. For example, a hybrid car-following strategy based on DDPG and Cooperative Adaptive Cruise Control (CACC) has been proposed [30]. By simultaneously calculating actions for both DDPG and CACC at each frame and selecting the optimal action, the proposed strategy significantly improves car-following performance across the entire state space. In addition, a DDPG-based car-following model with enhanced generalization capabilities was developed in [31]. This model, trained using an Ornstein-Uhlenbeck process for generating leader trajectories, demonstrated string stability and crash-free behaviour in extreme situations, further highlighting DDPG's robustness in complex scenarios. Furthermore, Qin et al. [29] introduced a DDPG-based car-following model that integrates both longitudinal and lateral control, addressing the issue of vehicle stability on curved roads. Their results demonstrated that the DDPG and Multi-Agent DDPG (MADDPG) models significantly enhance safety, comfort, and traffic flow efficiency compared with human driving. It highlights the ability of DDPG model in optimizing both longitudinal and lateral control, signif-

icantly reducing the lateral offset and improving stability under curved road conditions.

One of the most representative work on car-following based on DDPG is found in [17], which will be referred to as Zhu's model henceforth. An RL agent learns to control vehicle speed through trial and error in a simulation environment. To prevent potential unsafe actions, the model included a collision avoidance strategy during both training and testing phases, ensuring fast convergence and zero collisions. However, further investigation in [25] revealed that Zhu's model exhibited poor following comfort across multiple datasets containing real-world car-following events. Furthermore, despite achieving zero collisions, it showed high safety risks in some datasets.

III. DESCRIPTION OF ZHU'S MODEL

We shall first provide a description of the key components and implementation details of the Zhu's model.

A. REINFORCEMENT LEARNING MODEL

The DDPG algorithm used in Zhu's model includes an actor-critic mechanism. Two separate neural networks are used to approximate the policy (actor) and the value function (critic), respectively. The actor network is responsible for generating acceleration control strategies, while the critic network evaluates the current policy's performance and guides its improvement.

B. STATE AND ACTION

At each time step (t), the state of the car-following process consists of three components:

- Following vehicle speed $V_n(t)$
- Clearance distance $S_{n,n-1}(t)$
- Relative speed $V_{n,n-1}(t)$

The action is the longitudinal acceleration of the following vehicle $a_n(t)$. Based on the current state and action, the next state is updated through a kinematic model.

C. REWARD FUNCTION

The design of the reward function is central to this model. It is constructed by referencing human driving data and combining features related to driving safety, efficiency, and comfort. The reward function $r(s,a)$ consists of a linear combination of the following three features – safety, efficiency, and comfort.

1) Safety Feature

TTC is the time before a collision occurs, assuming the lead and following vehicles persists with the current speed. It is given by

$$\mathrm{TTC} = \frac{S_{n,n-1}(t)}{V_{n,n-1}(t)} \tag{1}$$

To penalize near-collision situations, the safety feature is expressed as

$$F_{\mathrm{TTC}} = \begin{cases} \log(\mathrm{TTC}) - \log(4) & \mathrm{TTC} < 4 \\ 0 & \mathrm{TTC} \geq 4 \end{cases} \tag{2}$$

2) Efficiency Feature

The headway time (THW) is defined as the time required for the following vehicle to reach a certain point ahead after the leading vehicle has passes it. Mathematically, it is given by

$$\mathrm{THW} = \frac{S_{n,n-1}(t)}{V_n(t)} \tag{3}$$

The efficiency feature is expressed as the probability density function of the headway time fitted to a log-normal distribution:

$$F_{\mathrm{headway}} = f_{\mathrm{lognorm}}(\mathrm{headway}; \mu = 0.4226, \sigma = 0.4365) \tag{4}$$

3) Comfort Feature

Jerk is measured by the rate of change of acceleration a. That is,

$$\mathrm{jerk} = \frac{da}{dt} \tag{5}$$

The comfort feature is defined as

$$F_{\mathrm{jerk}} = \frac{\mathrm{jerk}^2}{3600} \tag{6}$$

The reward function is expressed as a combination of the above three features:

$$r(s,a) = w_1 F_{\mathrm{TTC}} + w_2 F_{\mathrm{headway}} + w_3 F_{\mathrm{jerk}} \tag{7}$$

where the weights w_1, w_2, and w_3 are set to 1.

D. COLLISION AVOIDANCE STRATEGY

Although the reward function already includes penalties for small TTC values, to further ensure safety, Zhu's model incorporated a kinematic-based collision avoidance strategy. This strategy computes a safe following distance d_{safe}, given by

$$d_{\mathrm{safe}} = V_n \cdot \mathrm{RT} + \frac{V_n^2}{2a_{\max}} \tag{8}$$

where the reaction time (RT) is set to 1 second, and the maximum deceleration $a_{\max}$ is set to 3 m/s^2. When the following distance is less than d_{safe}, the vehicle applies emergency braking; otherwise, it follows the DDPG model's output acceleration.

IV. PROPOSED METHOD

In this paper, we proposed improved safety and comfort features for the reward function. The original safety feature f_{TTC}, based on a static TTC threshold, is not well-suited for real-world dynamic car-following scenarios. Additionally, according to the TTC calculation, when vehicle speeds are high and relative speeds are close, the TTC value can still be large despite small following distances, introducing potential safety hazards in the TTC-based safety feature. To

address these issues, a safety feature f_{safe} based on real-time headway time is proposed, enhancing the robustness of the car-following algorithm and avoiding the pitfalls of the TTC-based safety feature.

Furthermore, based on the research by Chen et al. [25], the car-following model proposed by Zhu et al. [17] exhibits poor performance in terms of comfort, indicated by high jerk values. Therefore, this study also introduces a jerk suppression to improve car-following comfort by limiting the acceleration/deceleration rates.

A. SAFETY FEATURE

As discussed earlier, the calculation equation (3) and significance of headway time have been outlined. To further enhance safety, this study implements the following improvement steps:

1) Defining Dynamic Safe Car-Following

Dynamic safe car-following is defined as the scenario where the following vehicle, with a speed greater than the leading vehicle, can decelerate to match or fall below the leading vehicle's speed based on the current gap, resulting in a relative speed of less than or equal to 0 m/s. The relative speed can be calculated using the following equation:

$$\triangle V = V_B - V_A \tag{9}$$

where ΔV is the relative speed, V_B is the speed of the following vehicle, and V_A is the speed of the leading vehicle.

2) Defining and Calculating Dynamic Safe Headway Threshold

The dynamic safe headway threshold is defined as the headway value corresponding to the maximum speed of the following vehicle that ensures dynamic safe car-following, given the current following distance and the maximum deceleration of the following vehicle.

The following is the procedure for calculating the dynamic safe headway threshold:

Given the current speed and deceleration of the vehicle, the braking distance D can be calculated as follows:

$$D = \frac{V^2}{2 * a} \tag{10}$$

where D is the braking distance, V is the current speed, and a is the deceleration.

By introducing the relative speed from Equation (9), the braking distance required for the following vehicle to decelerate to the same speed ($\triangle V = 0$) as the leading vehicle in a car-following scenario, given the current speeds and deceleration of both vehicles, can be calculated:

$$D_{safe} = \frac{\triangle V^2}{2 * a_B} \tag{11}$$

whereD_{safe} is the braking distance required to achieve dynamic safe car-Following, and a_B is the deceleration of the following vehicle.

Based on Equation (11) and Equation (9), by introducing the current following distance d and the maximum deceleration of the following vehicle $a_{\max}$, the upper limit of the following vehicle's speed ensuring dynamic safe car-following under the current following distance can be calculated as follows:

$$V_B = \sqrt{2 * a_{\max} * d} + V_A \tag{12}$$

where V_B is the upper limit of the following vehicle's speed, $a_{\max}$ is the maximum deceleration of the following vehicle, d is the current following distance, and V_A is the speed of the leading vehicle.

Finally, by substituting the current following distance d and the upper limit of the following vehicle's speedV_B into the headway time calculation equation (3), the dynamic safe headway threshold can be obtained:

$$H_t = \frac{d}{V_B} \tag{13}$$

The equation is expanded as:

$$H_t = \frac{d}{\sqrt{2 * a_{\max} * d} + V_A} \tag{14}$$

where H_t is the dynamic safe headway threshold.

3) Reward Function

The reward function is improved to incorporate the redesigned safety feature based on real-time headway time. The new reward function $r(s,a)$ is defined as follows:

$$r(s,a) = w_1 F_{\text{safe}} + w_2 F_{\text{efficiency}} + w_3 F_{\text{comfort}}$$

- **Safety Feature F_{safe}**:

$$F_{\text{safe}} = \begin{cases} \log\left(\frac{H}{H_T}\right) & \text{if } 0 < H < H_T \\ 0 & \text{if } H \geq H_T \\ -1 & \text{if } H \leq 0 \end{cases}$$

  where H is the current headway time, and H_T is the dynamic safe headway threshold calculated as follows:

$$H_T = \frac{S}{\sqrt{2 \cdot S \cdot a_{\max}} + V_A}$$

  where S is the current following distance, V_A is the speed of the leading vehicle, V_B is the speed of the following vehicle, and $a_{\max} = 3$ is the maximum deceleration.

- **Efficiency Feature $F_{\text{efficiency}}$**:

$$F_{\text{efficiency}} = f_{\text{lognorm}}(\text{headway}; \mu = 0.4226, \sigma = 0.4365)$$

  representing the headway time distribution fitted to a log-normal distribution.

- **Comfort Feature F_{comfort}**:

$$F_{\text{comfort}} = \frac{\text{jerk}^2}{3600}$$

  where jerk is the rate of change of acceleration.

The weights w_1, w_2, w_3 are hyperparameters that can be adjusted to balance the importance of safety, efficiency, and comfort.

B. JERK SUPPRESSION

The concept of comfort zones was introduced in [32]. The range of acceleration/deceleration was divided into three zones as shown in Table 1. Here, a represents the rear vehicle's acceleration/deceleration, $a_{\max}$ is its maximum acceleration/deceleration, d is the distance between the front and rear vehicles, V_B is the rear vehicle's speed, a_c is the comfortable acceleration/deceleration threshold (set to $2m/s^2$), u is the coefficient of friction, and g is the gravitational acceleration.

TABLE 1. Comfort Zones for Rear Vehicle as defined in [32]

Zone	Vehicle Separation	Acceleration
Comfort	$d > \left(\frac{V_B^2}{2a_c} - \frac{V_B^2}{2ug}\right)$	$a < a_c$
Discomfort	$\frac{V_B^2}{2a_{\max}} \leq d \leq \left(\frac{V_B^2}{2a_c} - \frac{V_B^2}{2ug}\right)$	$a_c \leq a < a_{\max}$
Dangerous	$d \leq \frac{V_B^2}{2a_{\max}}$	$a > a_{\max}$

It was argued that the rear vehicle needs to have its speed reduced to $0m/s$ in order to ensure that no collision will occur. This leads to the range of distances separating the two vehicles as shown in the middle column of Table 1. Based on this concept, we introduce two strategies for jerk reduction which are referred to as static and dynamic jerk reduction.

1) Static Jerk Suppression

Assume that initially the vehicles are travelling at the same speed such that $V_A = V_B$. If the leading vehicle decelerates, to avoid collision, the rear vehicle must reduce its speed to match that of the leading vehicle. Since now $V_A < V_B$, the time it takes to achieve $V_A = V_B$ is given by

$$t = \frac{V_B - V_A}{a_{B\_max}} \tag{15}$$

assuming that the deceleration of vehicle B is constant, denoted by a_{B_max}. This represents the maximum safe deceleration allowed. The distance traveled by Vehicle B is thus

$$d_B = V_B \cdot t - \frac{1}{2} a_{B\_max} \cdot t^2 \tag{16}$$

It can be expanded to

$$d_B = V_B \left(\frac{V_B - V_A}{a_{B\_max}}\right) - \frac{1}{2} a_{B\_max} \left(\frac{V_B - V_A}{a_{B\_max}}\right)^2 \tag{17}$$

$$= \frac{V_B^2 - V_A^2}{2a_{B\_max}} \tag{18}$$

We call this distance the absolute safety distance:

$$d_{safe} = d_B \tag{19}$$

Using this d_{safe}, the vehicle separation in Table 1 in the comfort zone could now be updated to that shown in Table 2. This is computed based on an acceleration/deceleration threshold a_c of $2m/s^2$ as before. We further propose a more comfortable interval referred to as the smooth zone. In this zone, the acceleration/deceleration threshold a_s is set to $1m/s^2$ to further limit the range of acceleration and deceleration to achieve further reduce jerk. The parameters of the smooth zone are shown in Table 2. Here, a represents the current acceleration or deceleration value of the rear vehicle. In the sequel, we shall refer to this jerk reduction strategy as *static*.

TABLE 2. Proposed Comfort and Smooth Zones

Zone	Quantity	Acceleration
Smooth	$d > (V_B^2 - V_A^2)/2a_s$	$a < a_s$
Comfort	$(V_B^2 - V_A^2)/2a_s > d > (V_B^2 - V_A^2)/2a_c$	$a_s \leq a < a_c$

2) Dynamic Jerk Suppression

With the static jerk suppression method above, the thresholds for the comfort and smooth zones are fixed. A Dynamic jerk suppression method could be formulated by making this threshold a_d dependent on the current spacing d between the front and rear vehicles and Equation (19). This threshold is given by

$$a_d = \frac{V_B^2 - V_A^2}{2d} \tag{20}$$

If the current deceleration a is less than this threshold, the system automatically limits the deceleration to the threshold deceleration a_d, ensuring that jerk remains within safe bounds. This real-time adjustment minimizes sudden changes in deceleration, thereby enhancing ride comfort and maintaining safety. Additionally, the dynamic nature of this strategy allows the autonomous vehicle to tighten or relax deceleration constraints as needed, adapting to the ever-changing traffic conditions and ensuring a balance between safety and comfort.

V. EXPERIMENTAL SETUP

A. DATASETS

This study employs two high-quality driving datasets: NGSIM I-80 [33] and HighD [21]. These datasets offer a diverse range of car-following scenarios to ensure generalizability and performance in various road environments and traffic conditions. NGSIM I-80 consists of 1,341 car-following episodes. Througout each episode, both the leading and following vehicles stay in the same lane. The duration of each one is longer than 15 seconds to ensure enough data points were captured to reflect meaningful car-following dynamics and enable robust statistical analysis.

HighD, released by the Institute of Automotive Engineering at RWTH Aachen University in Germany, contains driving dataset with bird's-eye view videos of six different roads around Cologne, Germany. Since they were captured by a high-resolution camera mounted on a drone, it provides high-precision positions and speeds of each vehicle, with positioning error under 10 cm.

In our study, 70% of NGSIM I-80 data were randomly selected for model training and the remaining 30% for testing.

A total of 1,881 car-following events, each lasting 15 seconds, were selected from HighD for testing purposes only.

B. BASELINE MODEL

The baseline model that is used for comparison is Zhu's model with the following key parameters:

- *The learning rate is set to* 0.001*, and the discount factor is* 0.90*.*
- *Exploration noise is generated using an Ornstein-Uhlenbeck process with parameters* $\theta = 0.15$ *and* $\sigma = 0.2$*.*
- *The state representation includes the following vehicle's speed, clearance distance, and relative speed.*
- *The action space consists of continuous control of longitudinal acceleration.*
- *Equal weighting for the three features – safety, efficiency and comfort, is used.*

VI. EXPERIMENTS AND RESULTS

A. SAFETY FEATURE EVALUATION

To assess the effectiveness of the proposed dynamic headway time alone, five independent models with this safety feature were trained using NGSIM I-80. At the same time, five baselines models are also trained. Two metrics are used to quantify the safety performance of the models: average number of collisions and collision rate. These metrics are commonly used in simulation studies, as supported by prior research [34], [17], where collision statistics serve as a practical means to evaluate and improve the safety performance of autonomous driving models. They provide a quantitative measure of a model's ability to avoid potential accidents. It is important to note that collisions in these simulations do not correspond directly to real-world traffic accidents but serve as indicators of safety performance in a controlled environment. By analyzing collision occurrences in simulation, we can identify weaknesses in the model's decision-making process and make necessary adjustments without posing real-world risks. The average number of collision is given by

$$\textit{Average Collisions} = \frac{\textit{Total Collisions}}{\textit{Total Number of Models}} \tag{21}$$

and the collision rate is calculated as

$$\textit{Collision Rate} = \frac{\textit{Models Involved in Collisions}}{\textit{Total Number of Models}} \tag{22}$$

Using the test data from NGSIM I-80, both the baseline and the proposed model did not produce any collision. However, as some random variations in the leading vehicle's speed are introduced, collisions start to occur. Table 3 shows the best and worst performances as the range of the leading vehicle's speed increased by 10% to 90%. Results of the best case are also illustrated graphically in Figure 1 and Figure 2. With the range of speed varying by up to 50% of the original, models with the new safety feature continued to achieve zero collisions for both cases. These results indicate that the proposed safety feature is more robust compared to the baseline.

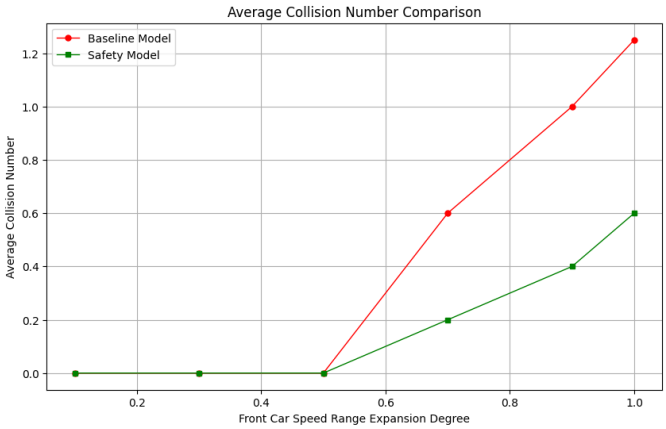

FIGURE 1. Average number of collisions as the range of leading vehicle's speed changes (Best case)

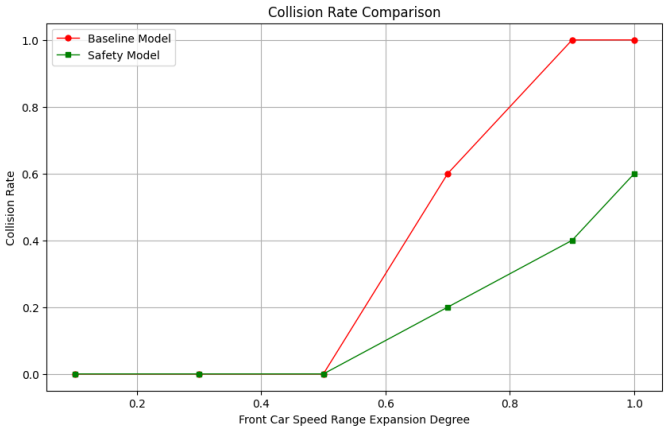

FIGURE 2. Collision rate as the range of leading vehicle's speed changes (Best case)

B. COMFORT FEATURE EVALUATION

Models incorporating jerk suppression are similarly trained. The average and the best jerk values achieved by each category of models are shown in Table 4. Static jerk suppression reduced the average jerk value by approximately 12% of the baseline. Dynamic jerk suppression, on the other hand, consistently achieved lower jerk values across all test conditions, reducing the average jerk value by about 19%. These results indicate that the proposed jerk suppression enhances driving comfort. The dynamic strategy, with its more precise control, effectively minimized sudden acceleration changes during driving. However, it is important to note that dynamic jerk suppression, by directly limiting the acceleration range, may result in lower following speeds. This is reflected in the increased headway time as shown in Table 5.

While models using jerk suppression alone improve riding comfort, they tend to exhibit a higher susceptibility to collision when tested across datasets. This implies that while the strategy excels in enhancing comfort, there may be safety trade-offs that need further optimization. This problem can be solved by combining the dynamic safety feature with jerk

TABLE 3. Collision statistics as the range of leading vehicle's speed range changes

Model	Speed Range Expansion	Avg Collisions Best	Avg Collisions Worst	Collision Rate Best	Collision Rate Worst
Baseline	0.1 (min: 2.64 m/s, max: 27.45 m/s)	0.0	0.2	0.0	0.2
	0.3 (min: 2.05 m/s, max: 32.44 m/s)	0.0	0.2	0.0	0.2
	0.5 (min: 1.47 m/s, max: 37.44 m/s)	0.0	2.4	0.0	1.0
	0.7 (min: 0.88 m/s, max: 42.43 m/s)	0.6	17.4	0.6	1.0
	0.9 (min: 0.29 m/s, max: 47.43 m/s)	1.0	47.2	1.0	1.0
New Safety Feature	0.1 (min: 2.64 m/s, max: 27.45 m/s)	0.0	0.0	0.0	0.0
	0.3 (min: 2.05 m/s, max: 32.44 m/s)	0.0	0.0	0.0	0.0
	0.5 (min: 1.47 m/s, max: 37.44 m/s)	0.0	0.0	0.0	0.0
	0.7 (min: 0.88 m/s, max: 42.43 m/s)	0.2	17.0	0.2	1.0
	0.9 (min: 0.29 m/s, max: 47.43 m/s)	0.4	46.0	0.4	1.0

TABLE 4. Vehicle Comfort Performance Analysis

Model	Average Jerk (m/s^3)	Lowest Jerk (m/s^3)
Baseline Model	0.84	0.63
Static Jerk Suppression	0.74	0.60
Dynamic Jerk Suppression Model	**0.68**	**0.57**

suppression.

TABLE 5. Headway Increase with Jerk Suppression

Model	Headway Time (s)	Jerk (m/s^3)
Baseline Model	**1.24**	0.63
Static Jerk Suppression Model	1.27	0.60
Dynamic Jerk Suppression Model	1.52	**0.57**

C. COMBINED DYNAMIC SAFE-FOLLOWING AND JERK SUPPRESSION

When dynamic safe-following and jerk suppression are combined, a significant improvement in overall driving performance is achieved. This combination resulted in zero collisions, a headway of 1.21 seconds, and a jerk value of 0.57 m/s^3, as shown in Table 6. In comparison, Zhu's model, which also produced zero collisions, recorded a headway of 1.24 seconds and a jerk value of 0.63 m/s^3. This suggests that the combined strategy not only reduces jerk but also enhances efficiency by achieving a slightly shorter headway, while maintaining safety.

The reason for this improvement lies in the complementary nature of the two strategies. The dynamic safe following strategy provides more precise adjustments to the following distance and speed based on real-time conditions, resulting in better control over acceleration and deceleration. This precision improves vehicle behaviour and reduces the need for larger headway. As a result, the combined strategy successfully mitigates the increase in headway observed when jerk suppression is used alone, achieving a better balance between comfort and efficiency.

TABLE 6. Performance of Dynamic Safe-Following with Jerk Suppression

Model	Headway Time (s)	Jerk (m/s^3)
Baseline Model	1.24	0.63
Dynamic Safe-Following + Jerk Suppression	**1.21**	**0.57**

D. GENERALIZATION ACROSS DATASETS

In order to assess the generalization ability of the models trained with the NGSIM dataset, it is tested against the HighD dataset. To ensure a robust comparison, five models of each configuration was trained separately under identical conditions to account for potential variability in the results. The following three different configurations are used:

1) ***DDPG (Baseline Model)**: Building on the DDPG algorithm proposed by Zhu et al., this approach integrates both safety and comfort strategies.*
2) ***DDPG + Dynamic_RE**: A dynamic headway threshold strategy is incorporated into the DDPG algorithm to improve the robustness of the following model.*
3) ***DDPG + Dynamic_RE + Jerk_Limitation**: Additionally, jerk suppression is incorporated into the previous configurations, aiming to minimize acceleration changes and enhance driving comfort.*

Two metrics are used to compare these configurations:

- ***Average Collisions**: This is defined by Equation (21*
- ***Collision Frequency (CFR)**: This metric represents the ratio of average collisions to the total number of test cases and is given by*

$$CFR = \frac{Average\ Collisions}{Total\ Number\ of\ Test\ Cases}$$

Table 7 shows the experimental results. For the "DDPG" and "DDPG+Dynamic_RE" configurations, the average number of collisions are 15 and 8.5 respectively, out of the 1881 test cases in the HighD dataset. The corresponding collision frequencies are 0.008 and 0.0045. Thus, by incorporating the dynamic headway threshold strategy, the model significantly reduced the collision rate. This further demonstrates the effectiveness and generalization capability of the strategy in enhancing safety across different driving conditions.

TABLE 7. Generalization Analysis on HighD Dataset

Algorithm	Average Collisions	Collision Frequency Rate (CFR)
DDPG (Baseline Model)	15	0.008
DDPG+Dynamic_RE	**8.5**	**0.0045**
DDPG+Dynamic_RE+Jerk_Limitation	43.25	0.023

When jerk suppression is introduced (DDPG + Dynamic_RE + Jerk_Limitation), both the average number of collisions and the collision rate increased slightly. The reason is that this strategy promotes more conservative acceleration decisions, potentially slowing response time during emergencies.

VII. CONCLUSIONS AND FUTURE WORK

In this paper, an improved method that guarantee safety and improve comfort for a DDPG-based reinforcement learning car-following model was proposed and validated. This method combines make use of a novel headway measure that is speed-dependent. The jerk suppression method is also dynamically adjusted depending on the spacing between the front and rear vehicles. Rigorous validation was performed with the NGSIM I-80 and HighD datasets. It showed significant improvements in both safety and driving comfort. The dynamic headway strategy effectively reduced collision rates, and is robust under varying driving conditions. Furthermore, dynamic jerk suppression was able to minimize the rate of acceleration changes, resulting in smoother riding experiences.

Further research could investigate our method's effectiveness in a wider range of driving scenarios. Such scenarios could include congested driving environments with frequent stops and starts.

REFERENCES

[1] X. Qu, Y. Yu, M. Zhou, C.-T. Lin, and X. Wang, "Jointly dampening traffic oscillations and improving energy consumption with electric, connected and automated vehicles: a reinforcement learning based approach," *Applied Energy*, vol. 257, p. 114030, 2020.

[2] J. Wang, L. Zhang, D. Zhang, and K. Li, "An adaptive longitudinal driving assistance system based on driver characteristics," *IEEE Transactions on Intelligent Transportation Systems*, vol. 14, no. 1, pp. 1–12, 2012.

[3] J. Olstam and A. Tapani, "Comparison of car-following models, swedish national road and transport research institute," *Project VTI meddelande*, vol. 960, 2004.

[4] L. A. Pipes, "An operational analysis of traffic dynamics," *Journal of applied physics*, vol. 24, no. 3, pp. 274–281, 1953.

[5] D. C. Gazis, R. Herman, and R. B. Potts, "Car-following theory of steady-state traffic flow," *Operations research*, vol. 7, no. 4, pp. 499–505, 1959.

[6] D. C. Gazis, R. Herman, and R. W. Rothery, "Nonlinear follow-the-leader models of traffic flow," *Operations research*, vol. 9, no. 4, pp. 545–567, 1961.

[7] M. Bando, K. Hasebe, A. Nakayama, A. Shibata, and Y. Sugiyama, "Dynamical model of traffic congestion and numerical simulation," *Physical review E*, vol. 51, no. 2, p. 1035, 1995.

[8] M. Treiber, A. Hennecke, and D. Helbing, "Congested traffic states in empirical observations and microscopic simulations," *Physical review E*, vol. 62, no. 2, p. 1805, 2000.

[9] T. V. Mathew and K. Ravishankar, "Neural network based vehicle-following model for mixed traffic conditions," *European Transport*, no. 52, 2012.

[10] A. Khodayari, A. Ghaffari, R. Kazemi, and R. Braunstingl, "A modified car-following model based on a neural network model of the human driver effects," *IEEE Transactions on Systems, Man, and Cybernetics-Part A: Systems and Humans*, vol. 42, no. 6, pp. 1440–1449, 2012.

[11] J. Morton, T. A. Wheeler, and M. J. Kochenderfer, "Analysis of recurrent neural networks for probabilistic modeling of driver behavior," *IEEE Transactions on Intelligent Transportation Systems*, vol. 18, no. 5, pp. 1289–1298, 2016.

[12] M. Zhou, X. Qu, and X. Li, "A recurrent neural network based microscopic car following model to predict traffic oscillation," *Transportation research part C: emerging technologies*, vol. 84, pp. 245–264, 2017.

[13] M. Li, Z. Li, S. Wang, and B. Wang, "Anti-disturbance self-supervised reinforcement learning for perturbed car-following system," *IEEE Transactions on Vehicular Technology*, vol. 72, no. 9, pp. 11 318–11 331, 2023.

[14] X. Zhang, J. Sun, Y. Wang, and J. Sun, "A hierarchical framework for multi-lane autonomous driving based on reinforcement learning," *IEEE Open Journal of Intelligent Transportation Systems*, vol. 4, pp. 626–638, 2023.

[15] S. Aradi, "Survey of deep reinforcement learning for motion planning of autonomous vehicles," *IEEE Transactions on Intelligent Transportation Systems*, vol. 23, no. 2, pp. 740–759, 2022.

[16] H. Dong, Z. Ding, S. Zhang, H. Yuan, H. Zhang, J. Zhang, Y. Huang, T. Yu, H. Zhang, and R. Huang, *Deep Reinforcement Learning: Fundamentals, Research, and Applications*, H. Dong, Z. Ding, and S. Zhang, Eds. Springer Nature, 2020, http://www.deepreinforcementlearningbook.org.

[17] M. Zhu, Y. Wang, Z. Pu, J. Hu, X. Wang, and R. Ke, "Safe, efficient, and comfortable velocity control based on reinforcement learning for autonomous driving," *Transportation Research Part C: Emerging Technologies*, vol. 117, p. 102662, 2020.

[18] M. H. Tawfeek and K. El-Basyouny, "A perceptual forward collision warning model using naturalistic driving data," *Canadian Journal of Civil Engineering*, vol. 45, no. 10, pp. 899–907, 2018.

[19] ——, "Location-based analysis of car-following behavior during braking using naturalistic driving data," *Canadian Journal of Civil Engineering*, vol. 47, no. 5, pp. 498–505, 2020.

[20] U.S. Department of Transportation Federal Highway Administration, "Next generation simulation (ngsim) open data," https://data.transportation.gov/stories/s/Next-Generation-Simulation-NGSIM-Open-Data/i5zb-xe34/, 2016.

[21] R. Krajewski, J. Bock, L. Kloeker, and L. Eckstein, "The highd dataset," https://www.highd-dataset.com, 2018.

[22] S. Hwang, K. Lee, H. Jeon, and D. Kum, "Autonomous vehicle cut-in algorithm for lane-merging scenarios via policy-based reinforcement learning nested within finite-state machine," *IEEE Transactions on Intelligent Transportation Systems*, vol. 23, no. 10, pp. 17 594–17 606, 2022.

[23] G. Wang, J. Hu, Z. Li, and L. Li, "Harmonious lane changing via deep reinforcement learning," *IEEE Transactions on Intelligent Transportation Systems*, vol. 23, no. 5, pp. 4642–4650, 2021.

[24] X.-M. Chen, M. Jin, Y.-s. Miao, and Q. Zhang, "Driving decision-making analysis of car-following for autonomous vehicle under complex urban environment," *Journal of central south university*, vol. 24, pp. 1476–1482, 2017.

[25] X. Chen, M. Zhu, K. Chen, P. Wang, H. Lu, H. Zhong, X. Han, X. Wang, and Y. Wang, "Follownet: a comprehensive benchmark for car-following behavior modeling," *Scientific data*, vol. 10, no. 1, p. 828, 2023.

[26] R. E. Chandler, R. Herman, and E. W. Montroll, "Traffic dynamics: studies in car following," *Operations research*, vol. 6, no. 2, pp. 165–184, 1958.

[27] V. Kurtc and M. Treiber, "Simulating bicycle traffic by the intelligent-driver model-reproducing the traffic-wave characteristics observed in a bicycle-following experiment," *Journal of traffic and transportation engineering (English edition)*, vol. 7, no. 1, pp. 19–29, 2020.

[28] J. Ren, "Car following model and algorithm design based on reinforcement learning," in *Journal of Physics: Conference Series*, vol. 2083, no. 3. IOP Publishing, 2021, p. 032008.

[29] P. Qin, H. Tan, H. Li, and X. Wen, "Deep reinforcement learning car-following model considering longitudinal and lateral control," *Sustainability*, vol. 14, no. 24, p. 16705, 2022.

[30] R. Yan, R. Jiang, B. Jia, J. Huang, and D. Yang, "Hybrid car-following strategy based on deep deterministic policy gradient and cooperative adaptive cruise control," *IEEE Transactions on Automation Science and Engineering*, vol. 19, no. 4, pp. 2816–2824, 2022.

[31] F. Hart, O. Okhrin, and M. Treiber, "Formulation and validation of a car-following model based on deep reinforcement learning," *arXiv preprint arXiv:2109.14268*, 2021.

[32] Z. Wu, Y. Liu, and G. Pan, "A smart car control model for brake comfort based on car following," *IEEE transactions on intelligent transportation systems*, vol. 10, no. 1, pp. 42–46, 2008.
[33] M. Montanino and V. Punzo, "Trajectory data reconstruction and simulation-based validation against macroscopic traffic patterns," *Transportation Research Part B: Methodological*, vol. 80, no. 1, pp. 82–106, 2015.
[34] A. Dosovitskiy, G. Ros, F. Codevilla, A. Lopez, and V. Koltun, "Carla: An open urban driving simulator," in *Conference on robot learning*. PMLR, 2017, pp. 1–16.

KE LIU received his Masters degree in Computer and Information Sciences from The University of Sydney, Sydney, Australia in 2022. He is now a PhD student at the Auckland University of Technology, Auckland, New Zealand.

JING MA (Member, IEEE) received the PhD degree in Computer Sciences from Auckland University of Technology, New Zealand, in 2019. She is currently a lecturer at the Department of Computer Science and Software Engineering at Auckland University of Technology, Auckland, New Zealand.

EDMUND M-K LAI (Life Senior Member, IEEE) received his BE(Hons) and PhD from The University of Western Australia, both in Electrical Engineering, in 1982 and 1991 respectively. He is currently Professor of Information Engineering at the Auckland University of Technology, New Zealand. He has over 35 years of academic experience, having previously held faculty positions at universities in Australia, Hong Kong, and Singapore. He has published over 150 international refereed journal and conference papers in signal processing, intelligent control, computational intelligence, and artificial neural networks. Dr. Lai is also a Fellow of the Institution of Engineering and Technology (FIET) and a Fellow of Engineers Australia (FIEAust).